Nitrogen doping and carbon coating affects substrate selectivity of TiO2 photocatalytic organic pollutant degradation

ARTICLE

Nitrogen doping and carbon coating affects substrate selectivity of TiO_2 photocatalytic organic pollutant degradation

Yishu Zhang, Caroline Kirk,* and Neil Robertson*[a]

[a] Y. Zhang, Dr. C. Kirk, Prof. N. Robertson
School of Chemistry
University of Edinburgh
Joseph Black Building
David Brewster Road, Edinburgh, EH9 3FJ
E-mail: neil.robertson@ed.ac.uk

Supporting information for this article is given via a link at the end of the document.

Abstract: A series of carbon-coated, nitrogen-doped titanium dioxide photocatalysts was produced and characterized. N-doped TiO_2 powder samples were prepared using a sol-gel method and subsequently used for making doped-TiO_2 thin films on glass substrates. Carbon layers were coated on the films by a thermal decomposition method using catechol. Diffuse reflectance spectra and Mott-Schottky analyses of the samples proved that nitrogen doping and carbon coating can slightly lower the band gap of TiO_2, broaden its absorption to visible light and enhance its n-type character. According to photocatalytic tests against model contaminants, carbon-coated nitrogen-doped TiO_2 films have better performance than simple TiO_2 on the degradation of Rhodamine B dye molecules, but are poorly effective for degrading 4-chlorophenol molecules. Several possible explanations are proposed for this result, supported by scavenging experiments. This reveals the importance of a broad substrate scope when assessing new photocatalytic materials for water treatment, something which is often overlooked in many literature studies.

Introduction

According to UN research, over 80% of wastewater is released to the environment without adequate treatment. The pollutants in wastewater are released into the water cycle, causing direct impacts on human health, the environment and economic productivity[1]. Only 8% of the municipal and industrial wastewater in low-income countries undergoes treatment such that people from those countries face the threat of water pollution because of a lack of water sanitation services[2]. Most methods of water treatment depend upon energy, land and budget being available around the clock, which is rarely the case in most developing countries. Low-tech and nature-based solutions also exist but usually do not guarantee a quality of water that is safe for drinking[3]. It is key therefore to develop small-scale, high-efficiency and low-cost methods of removing pollutants from drinking water.

Titanium dioxide (TiO_2), as a high-stability and non-toxic semiconductor material, has been used as a photocatalyst for degradation of contaminants in water. However, two limitations affect the photocatalytic efficiency of TiO_2. Although the wide band gap of more than 3.0 eV is suitable for producing reactive oxygen species, the usage of solar energy in TiO_2 photocatalysis is restricted to UV light, less than 5% of the total solar radiation[4]. Also, the fast recombination of photogenerated electrons and holes in TiO_2 means the rate of surface reactions taking place on the catalyst would be low[5]. Many developments have been made in TiO_2 photocatalysts according to recent research reports, including nanostructure modifications[6], band gap narrowing through doping[7], deposition of plasmonic metal nanoparticles[8] and the formation of composite materials with other inorganic semiconductors[9].

Doping TiO_2 with other atoms is a well-known method of changing the band gap and expanding the light absorption of the photocatalytic material. Dopant atoms can provide additional orbitals to create an intermediate band below the conduction band or above the valence band, and the band gap can be narrowed in general. The doped TiO_2 can capture photons with longer wavelength and lower energy, which means more solar energy can be utilized. Various metal and non-metal atoms have been used as dopants with TiO_2, such as Cu, Sn, Gd[10][11][12] and N, C, F[13][14][15], and the photocatalytic efficiency has been reported as higher than unmodified TiO_2.

Coating TiO_2 with a highly-conducting carbon layer to decrease charge recombination and increase visible light absorption, has been investigated in recent years. The carbon layer can accept the high energy electrons from electron-hole pairs photogenerated in TiO_2, thus increasing the efficiency of charge separation and photoreaction[16]. TiO_2-C hybrid materials improve the photocatalytic activity in reactions with organic molecules and metal ions in high oxidation states[16]. Besides, the carbon layer also provides chemical protection for TiO_2[17]. The stable, non-toxic and low-cost carbon layer is suitable for modifying photocatalysts designed for application in the natural environment.

Herein, we describe for the first time the preparation of carbon-coated nitrogen-doped TiO_2 thin film photocatalysts. Nitrogen doping and carbon coating increase absorption of solar energy and improve charge separation in the hybrid TiO_2 material such that it can achieve a higher photocatalytic efficiency. The whole preparation route was designed under the principle of being low-cost, non-toxic and environmentally-friendly. Sol-gel methods, the simplest approach for producing TiO_2 nanoparticles in the lab, were used to prepare N-doped TiO_2. Urea was chosen as the nitrogen source in the preparation route, and catechol was used for forming a carbon layer by a thermal decomposition route. Powder catalysts are difficult to collect and recycle after purifying

water samples, and nanoparticles may carry risk to human health and the environment when released to nature[18]. Immobilizing the modified-TiO_2 powder on glass substrates gives a simple route to collect and recycle the photocatalyst from solution. Photocatalytic tests were carried out against model contaminants, and the mechanism of photocatalytic reaction on the surface of our material was studied.

Results and Discussion

In this work, undoped TiO_2 and N-doped TiO_2 powder samples were prepared and labelled as T, T2N and T5N, where 2 and 5 were the molar ratio of urea added to the titanium tetrabutoxide ($Ti(OBu)_4$). Films of the three samples were then made and labelled as the same names. The films after carbon coating were labelled as TC, T2NC and T5NC.

Characterization

Scanning electron microscope (SEM) images of N-doped TiO_2 powder are shown in Figure 1. The particle size varies from 200 nm to 40 μm, and bulky particles were observed. SEM images show no obvious differences of particle shape and particle size between the pure TiO_2 sample and N-doped TiO_2 samples, suggesting that the formation of bulky particles is due to the general synthesis method instead of nitrogen doping.

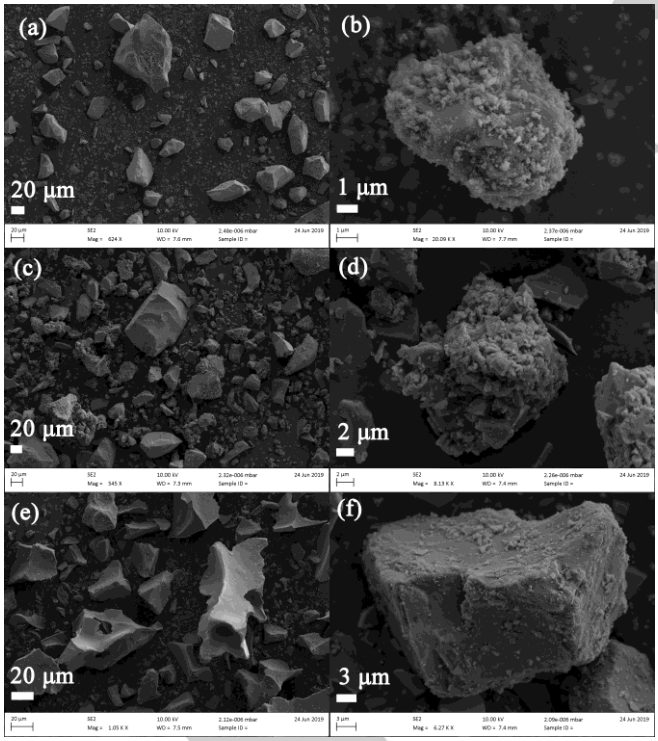

Figure 1. SEM images of (a)(b)T, (c)(d)T2N, (e)(f)T5N powder samples

X-ray Powder Diffraction (XRPD) patterns and UV-vis diffuse reflectance spectra (DRS) of the samples were measured after every step of the preparation route. Analysis of the XRPD patterns assigned all the observed peaks to that of anatase (ICSD #9852) with no indication of the presence of any other TiO_2 polymorph in quantities detectable by XRPD techniques (> 3 wt%). All the TiO_2 powder samples (Figure S1) were found to be well crystalline, with similar sharpness of peak widths, which may lead to the conclusion that nitrogen doping has little effect on the crystallization of anatase. The average crystallite size (L) of T, T2N and T5N powder samples were calculated using the peak observed at 2θ = 25.3° by the Scherrer equation (Eq. 1) and are listed in Table 1.

$$L = \frac{K\lambda}{\beta cos\theta} \quad (1)$$

where λ is the X-ray wavelength (Kα = 0.154184 nm), β is Full Width at Half Maximum (FWHM), and K is a constant related to crystallite shape, normally taken as 0.9[19]. Data were analysed using a pattern fitting algorithm and the peak positions and FWHM were determined using a pseudo-Voigt peak function. The datasets for the three samples were collected on the same diffractometer under the same conditions, reducing instrumental errors. Errors on these values are quoted in brackets in Table 1. According to the calculation results, the crystallite size decreased slightly with the increase of nitrogen included. Smirniotis *et al*. reported a slight peak shift caused by nitrogen doping[20], but there is no obvious peak shifts observed on comparison of these XRPD patterns. The crystallite size is much smaller than the particle size, suggesting that small nanoparticles have aggregated into a bulk, which causes a decrease of surface area, therefore the surface photocatalytic reaction efficiency is expected to be affected.

Table 1. Crystallite size of TiO_2 powder samples.

Sample	Crystallite size (nm)
T	17.2 (9)
T2N	16.3 (7)
T5N	14.6 (9)

The Tauc plots of powder samples are given in Figure 2 a. A tail of additional absorption in the area of 2.5 ~ 3.2 eV can be seen in the Tauc plot of N-doped TiO_2 samples, which is similar to previous reports of N-doped TiO_2 materials[21][22][23]. The additional absorption of light is in the visible region, which means nitrogen doping has expanded the solar energy absorption of TiO_2 to visible light, consistent with the samples taking on a pale-yellow appearance compared with white TiO_2. The absorption tail area of T5N is larger than that of T2N, showing that more nitrogen doping brings more visible light harvesting.

XRPD patterns of N-TiO_2 films (Figure S2) show that the doctor blading method does not alter the anatase structure of N-TiO_2. Similarly, the Tauc plot of N-TiO_2 film samples (Figure 2 b) shows that the light absorption of the powder samples is retained after forming the photocatalyst films.

Following carbon coating of these films by degradation of surface-adsorbed catechol, they were studied by powder XRD. The XRPD patterns of the C-coated TiO_2 films (Figure 3) show that sharp anatase peaks are still observed, proving that carbon coating has not altered the crystal structure of the TiO_2 phase. The broad bumps observed in the 2θ ranges = 7°- 15 and 20 - 35° may be due to the glass substrate. In keeping with the

characterization of C-coated material reported by Odling et al.[17], information about carbon layers was not observed in the XRPD pattern, which means carbon did not form a crystalline material.

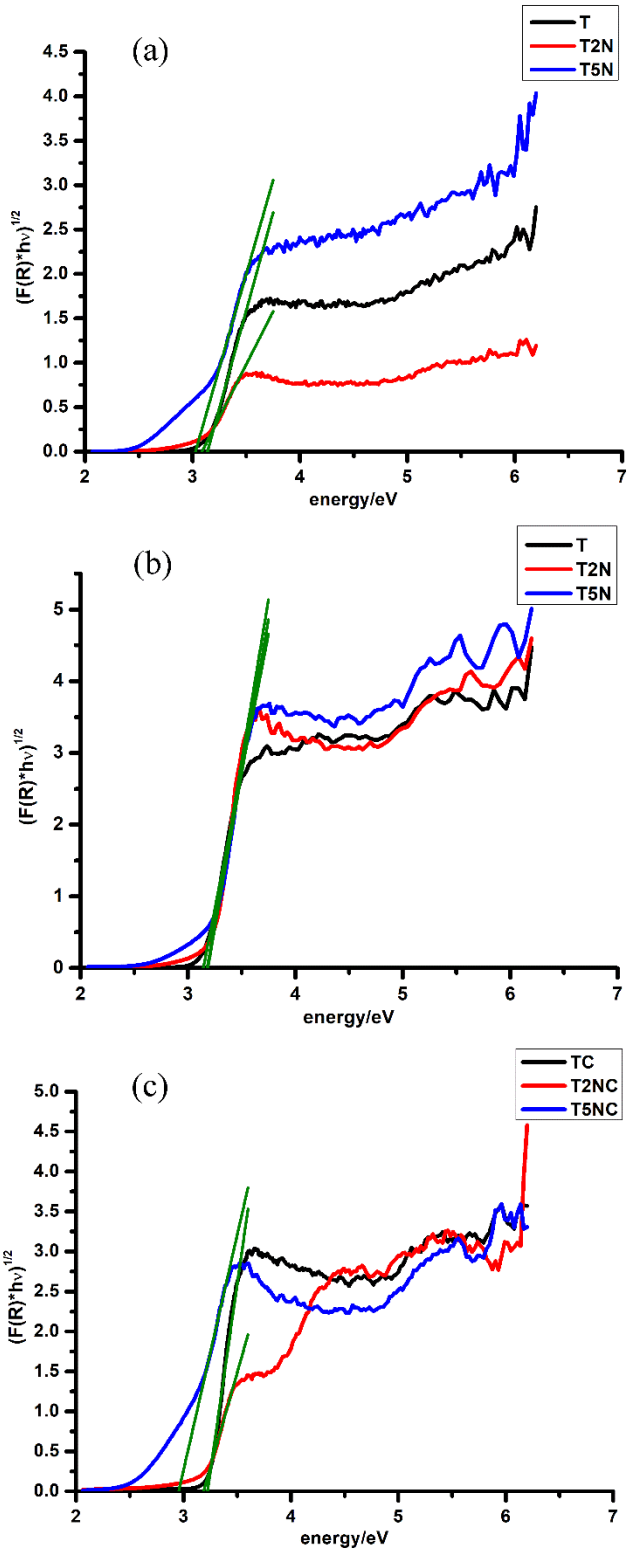

Figure 2. Tauc plots of powder samples (a), N-TiO_2 films (b) and C-coated films (c).

The additional absorption tail area can still be seen in the Tauc plots of T2NC and T5NC samples (Figure 2 c). The band gaps (E_g) of all 9 samples tested were determined for each sample from the x-axis of the Tauc plot according to the Tauc equation (Eq. 2) and are summarised in Table 2.

$$(F(R_\infty)h\nu)^{\frac{1}{n}} = A(h\nu - E_g) \quad (2)$$

where $F(R_\infty)$ is obtained from the Kubelka-Munk function[24]. The value of n in this case is 2 for indirect allowed transition[25]. According to the Tauc plots and the band gap values, nitrogen doping has extended the absorption of light, which can be seen in the Tauc plot as the tail area. Carbon coating has also slightly lowered the band gap of the material and expanded the light harvesting. Both modifications have increased the potential utilization of solar energy.

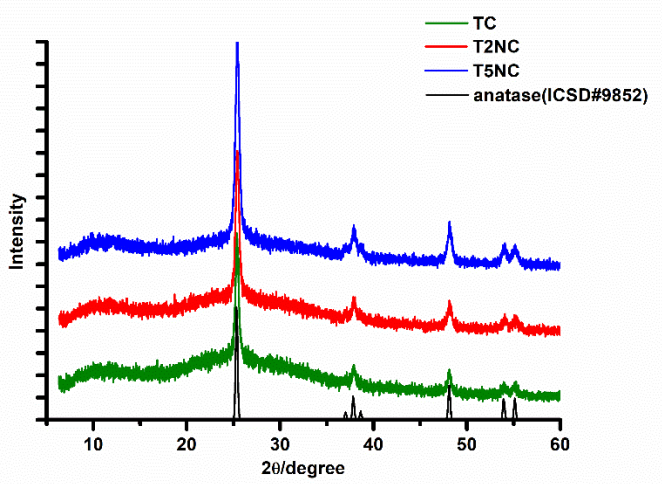

Figure 3. XRD patterns of C-coated N-TiO_2 film samples.

Table 2. Band gap of modified TiO_2 materials.

Sample	Band gap (eV)
T(powder)	3.14
T2N(powder)	3.09
T5N(powder)	3.03
T(film)	3.16
T2N(film)	3.18
T5N(film)	3.18
TC	3.22
T2NC	3.19
T5NC	2.96

Mott-Schottky plots of T and T5N thin films are shown in Figure 4. Mott-Schottky analysis is widely used to determine the flat band potential (E_{fb}) of semiconductor[26]. The linear portion of

the Mott-Schottky plots can be extrapolated to the x-axis to obtain a value for the E_{fb} according to the Mott-Schottky equation (Eq. 3)

$$\frac{1}{C^2} = \frac{2}{\varepsilon\varepsilon_0 A^2 e N_D}(E - E_{fb} - \frac{k_B T}{e}) \quad (3)$$

where ε is the dielectric constant of the material, ε_0 is the permittivity of free space, A is the interfacial area, N_D describes the charge carrier density, E describes the applied potential, k_B is the Boltzmann constant and T is the absolute temperature. Both of the plots have a positive gradient in the linear region, which is the typical n-type conductivity pattern. Comparing with undoped TiO_2, the flat band potential of T5N has a negative shift, indicating that nitrogen doping enhances the n-type conductivity of the material. This is consistent with previous research[23].

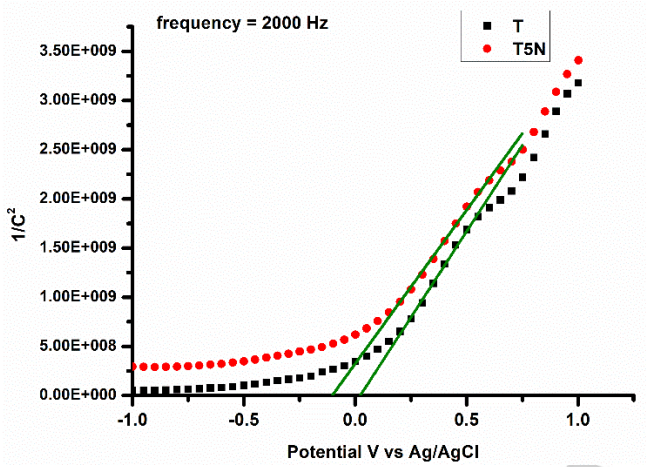

Figure 4. Mott-Schottky plot of T and T5N films.

In summary, nitrogen doping and carbon coating introduce an additional absorption of visible light to the TiO_2 materials. Nitrogen atoms doped into TiO_2 may bring additional states above the valence band, so that the electrons can be excited by photons with lower energy. Carbon coating also helps further expand the absorption of light by adding states below the conduction band[17] and is expected to also enhance charge separation.

Photocatalytic testing

The system for photocatalytic testing is shown in Figure 5. Rhodamine B and 4-chlorophenol were chosen as model pollutants for photocatalytic testing. Dye molecules (eg. methyl orange, methylene blue) are frequently used in testing semiconductor photocatalytic materials. However, only using dye molecules may lead to an incomplete picture of the photocatalytic performance. Excitation of the analyte dye by visible light, in addition to the photocatalyst, can increase rates significantly, and can make even undoped TiO_2 appear to be active under visible only irradiation.[17] In order to overcome the effect caused by self-sensitization of dyes, 4-chlorophenol, a colourless UV-absorbing molecule, was also used as another model contaminant. Control experiments, using a glass slide without photocatalyst, were also carried out against the two model pollutants. Based on the data of the control experiments, small concentration changes caused by solvent evaporation were corrected from the test results of all samples.

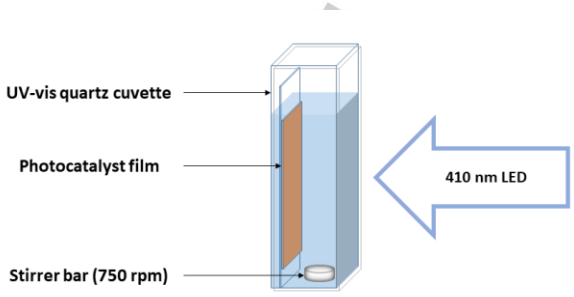

Figure 5. Photocatalytic test set-up.

The results of photocatalytic testing against Rhodamine B and the calculated pseudo-first-order rate plots are shown in Figure 6 and Figure S3. Pure TiO_2 cannot absorb 410 nm light, so the result of T sample shows that Rhodamine B didn't degrade by photolysis under 410 nm LED light in this system. The TC sample also shows no degradation, which means TiO_2 with only carbon coating and no N-doping is not able to absorb 410 nm light. The dropping absorption in the results of T2N, T5N, T2NC and T5NC were caused by photoreactions catalyzed by the modified TiO_2 films. All N-TiO_2 and C-N-TiO_2 films were effective in degrading Rhodamine B molecules, in which T5NC shows the best photocatalytic efficiency, approximately 40% after 3 hours. A summary of pseudo-first-order rate constants of T2N, T5N, T2NC and T5NC samples against Rhodamine B is given in Table 3.

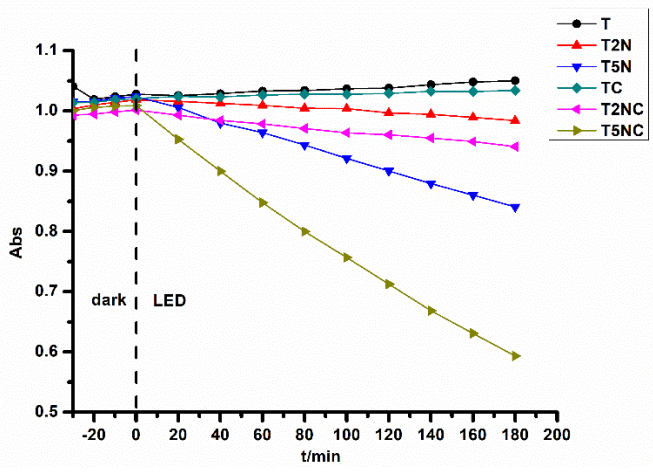

Figure 6. Testing of modified TiO_2 photocatalysts against Rhodamine B.

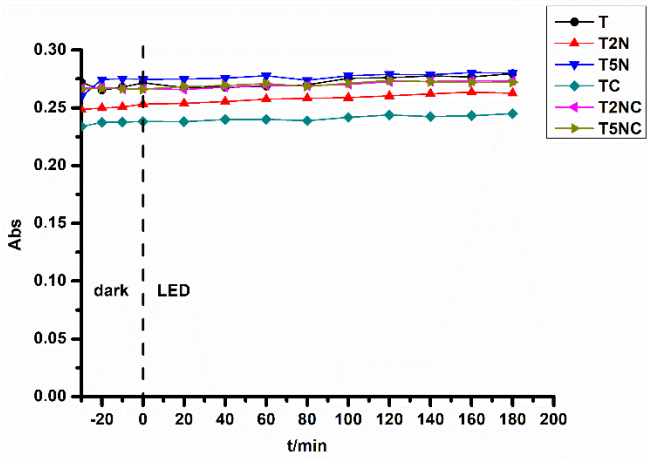

Figure 7. Testing of modified TiO2 photocatalysts against 4-chlorophenol.

Upon changing to the 4-chlorophenol model pollutant however (Figure 7), no photocatalytic degradation was observed from the test results of any sample, which indicates that 4-chlorophenol cannot be degraded in the system set-up of this work.

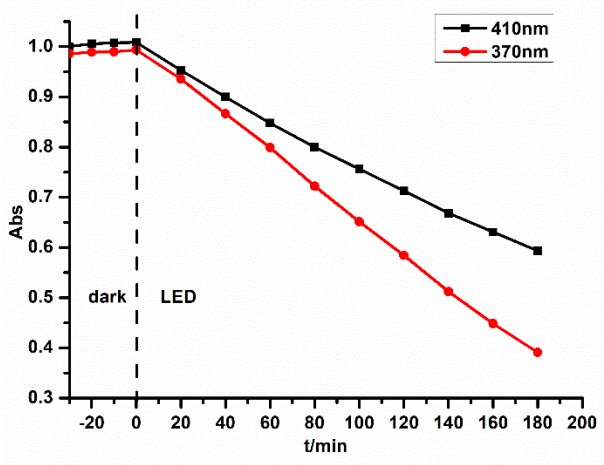

Figure 8. Testing of T5NC against Rhodamine B under 410 nm and 370 nm LEDs.

Table 3. Pseudo-first-order rate constant of TiO_2 samples against Rhodamine B.

Sample	Pseudo-first-order rate constant ($\times 10^{-3}$ min^{-1})
T2N	0.177
T5N	1.08
T2NC	0.351
T5NC	2.93

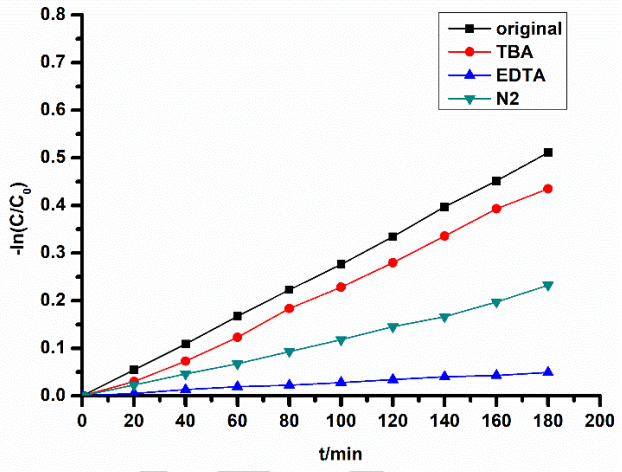

Figure 9. First order rate plot of scavenging tests using T5NC sample on the degradation of Rhodamine B.

Photocatalytic testing under UV light was also carried out using sample T5NC, and was compared with the 410 nm test result (Figure 8). The increased degradation efficiency (60.7%) showed that TiO_2 absorbs UV light well. These different test results taken together demonstrate that the modified TiO_2 photocatalyst is able to harvest UV and visible light, which is important for real-world application.

In order to study the mechanism of photocatalytic reaction happening on the C-N-TiO_2 material, scavenging experiments were done by removing key species from T5NC-Rhodamine B reaction system. Tert-butanol (TBA) is a scavenger of hydroxyl radicals, disodium EDTA can scavenge photogenerated holes at the photocatalyst surface, and degassing using N_2 can exclude O_2 from the solution, hindering the reduction of O_2 to the superoxide ion radicals.[17] The first order rate plot of scavenging tests (Figure 9) gives a clear comparison of reaction rates of those tests. The pseudo-first-order rate constants in scavenging experiments are given in Table 4.

Table 4. Pseudo-first-order rate constant in scavenging experiments.

Scavenger	Pseudo-first-order rate constant ($\times 10^{-3}$ min^{-1})
None	2.81
TBA	2.37
EDTA	0.28
N_2	1.23

It was found that the major species taking part in the photocatalytic reaction was photogenerated holes, with addition of EDTA causing an almost complete drop of reaction rate. Adding a high concentration of TBA only brought a slight drop of reaction rate, which indicates that •OH is a minor species in the photocatalytic system. Bubbling N_2 decreased the reaction rate more than 50%, showing that superoxide radicals also play an important role in the reaction, possibly due to recombination with

holes if they are not removed. A similar result was reported by Odling et al.[17] on the test of carbon coated Cl-TiO_2 materials made by the same carbon coating method.

The stability of C-N-TiO_2 photocatalyst was studied by UV-Vis diffuse reflectance spectra and recycling tests after the initial photocatalytic tests. Comparing with the Tauc plot before Rhodamine B degradation process, the Tauc plot after photocatalytic reaction shows a loss of additional absorption (Figure S4). Furthermore, according to the results of recycling tests using 370 nm LED, an increase of degradation efficiency appeared in the second cycle, showing that the photocatalyst film was changing during the first degradation process (Figure S5). In addition, some particles were seen to detach from the film after the test, likely due to the large particle size. Producing smaller particles of N-doped TiO_2 material may increase the photocatalytic performance and stability of modified TiO_2 thin films.

Table 5 gives a comparison of C-N-TiO_2 prepared in this work and some similar modified TiO_2 materials reported previously. These studies included photocatalysts which have a similar carbon layer on TiO_2, a similar preparation route, or the same anatase phase structure with C-N-TiO_2 prepared in this work. Several caveats are important when comparing outcomes from different studies. Firstly, many studies use only one dye molecule as model pollutant, which carries the risk of self-sensitization of the catalytic process through light-absorption by the dye and subsequent electron transfer to the TiO_2. In our work, we carried out tests additionally against the colourless 4-chlorophenol, giving results that are more representative of photocatalytic efficiency against general organic contaminants in the real world. Secondly, the light sources used have varying power levels, with typical high-power light sources (Xe lamp, halogen lamp, etc.) higher energy than LEDs used by us. Finally, photocatalysts immobilised on substrates, e.g. in our study, generally have lower photoreaction rate than powder photocatalysts because of the decrease of surface area and slower mass transport. These however benefit from ease of separation and recyclability and so are important for real-world use. Taking all these points into consideration, the rate performance of our materials broadly compares very favourably with similar literature materials in Table 5, while being mindful that the different experimental conditions precludes direct numerical comparison of rates.[27][28]

Within this context however, the lack of degradation of 4-chlorophenol is striking. The oxidation potentials of 4-chlorophenol and Rhodamine B measured by cyclic voltammetry (Figure S6) shows that 4-chlorophenol will oxidize at a higher potential than Rhodamine B. Since the nitrogen doping has brought extra states above the valence band of TiO_2, the photogenerated holes will be located at a less-positive electrochemical potential, which may be able to oxidize Rhodamine B but cannot oxidize 4-chlorophenol. An energy level diagram (Figure 10) represents this difference.

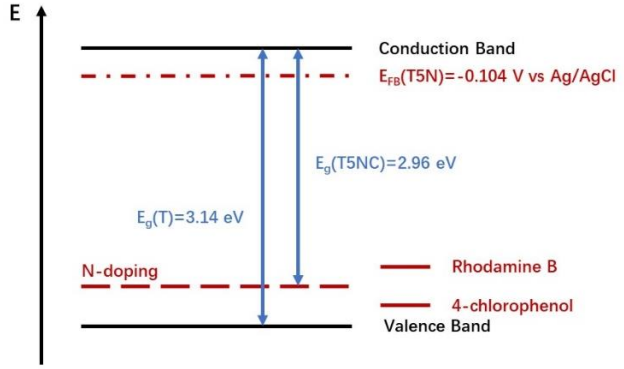

Figure 10. Energy level diagram of C-N-TiO_2 and model pollutant molecules.

Another possible explanation as to why the system can't degrade 4-chlorophenol is a potentially weaker molecule adsorption to the photocatalyst film. Since scavenging tests show that photogenerated holes are the main species in the photocatalytic reaction, organic molecules should be absorbed onto the surface of photocatalyst to react with the holes, which means less absorption leads to slow reaction rate. 4-chlorophenol molecules may be hard to absorb on the TiO_2 material, so being

Table 5. Recently Published N-doping or C-coating TiO_2 Photocatalyst Materials.

Material	Model Pollutant	Catalyst loading and Form	Light Source	Photocatalytic Degradation Measure
C-N-TiO_2 (this work)	Rhodamine B	Film on glass substrates in approx. 3 mL	4 W 410 nm LED	0.00293 min^{-1}
C-Cl-TiO_2 [17]	Methyl Orange (MO) 4-chlorophenol (4-CP)	Film on glass substrates in approx. 3 mL	30 W white LED (>400 nm)	0.0101 min^{-1} (MO) 0.00386 min^{-1} (4-CP)
N-TiO_2 [29]	Methyl Orange	0.5 g powder in 500 mL	300 W Xe Lamp (>400 nm)	96.6% degradation after 1.5 hours
N-TiO_2 [21]	Rhodamine B	20 mg powder in 20 mL	350 W Xe Lamp (≥420 nm)	90.3% degradation after 2 hours
N-TiO_2 [30]	p-nitrophenol	10 mg powder in 10 mL	300 W Halogen Lamp (>390 nm)	43% degradation after 24 hours
N-TiO_2 [31]	Methylene blue	Film on Ti foils in 50 mL	350 W Xe lamp (≥420 nm)	55% degradation after 2 hours

unable to react with the holes and therefore cannot be degraded. This explanation is less convincing however since neither molecule shows significant dark adsorption in the photocatalytic experiments before application of the light (Figure 6, Figure 7).

Another possibility is that the initial products of 4-chlorophenol degradation may be molecules similar to itself, with UV absorption peak overlapping with that of 4-chlorophenol. This is less likely to be the case with the more conjugated visible chromophore Rhodamine B. Again however, this explanation would appear unlikely due to the complete absence of significant spectral changes upon photocatalytic treatment of 4-chlorophenol (Figure S7).

Conclusion

Nitrogen doped carbon coated TiO_2 film photocatalysts were prepared and tested against two model pollutants in water. It was demonstrated that nitrogen doping and carbon coating expand the solar energy absorption of TiO_2, making the material able to use energy from visible light. Photocatalytic test results show that the combination of doping with nitrogen and coating with a carbon layer gave the best performance in TiO_2 modification for degradation of Rhodamine B. Mechanistic studies indicate that photogenerated holes and superoxide radicals are the main species participating in the photocatalytic reaction. Although the photocatalytic system showed a good performance on degrading Rhodamine B, it showed no capability to degrade 4-chlorophenol, which may be most likely explained by the less-positive hole potential of modified TiO_2. This finding emphasizes the central importance of using a varied scope of model pollutants when assessing new photocatalytic materials. Many literature studies use only a coloured dye as test molecule and on this basis, broad applicability of the catalyst to organic pollutants cannot be claimed.

Experimental Section

Chemicals

Titanium tetrabutoxide, urea, acetyl acetone and acetic acid were purchased from Sigma-Aldrich. Ethanol was purchased from Fischer. Triton X-100 was purchased from Acros Organics.

N-doped TiO_2 powder preparation

Pure ethanol (6.5 mL), pure acetic acid (1 mL) and acetyl acetone (0.5 mL) were mixed together and titanium tetrabutoxide (5 mL) was added slowly into the mixture under continuous stirring to form Solution A. Urea (1.7612 g for T2N sample, 4.4030 g for T5N sample) was dissolved in ultrapure water (8 mL for T2N sample, 20 mL for T5N sample in order to dissolve urea completely). Then ethanol (12 mL) and acetic acid (12 mL) were added into the urea solution to form Solution B. For the undoped (T) sample, Solution B only contained ultrapure water (8 mL), ethanol (12 mL) and acetic acid (12 mL). After stirring Solution A for 30 min, Solution B was added dropwise into Solution A during continuous stirring. The mixture was stirred for a further 30 min and then dried on a hot plate under air at 100℃ overnight. After grinding, the solid sample was annealed in a furnace at 500℃ for 2 h.

Film formation

Deionized water (2 mL) was dropped into N-doped TiO_2 powder (0.5 g) under stirring. Acetyl acetone (0.1 mL) and Triton X-100 (1 drop) were then added before stirring overnight to make the N-doped TiO_2 paste.

Microscope glass slides were cut into 3.75 cm * 0.9 cm rectangles before ultrasonic cleaning in a solution of detergent (Decon 90, ≈5% in tap water) for 15 min. The substrates were then scratched by sand paper on one side and then ultrasonically cleaned with 5% detergent, tap water, deionised water and finally ethanol for 15 min each step. Finally, the glass slides were treated with UV-ozone cleaner for 15 min. The N-doped TiO_2 paste was then doctor bladed in 3 cm * 0.9 cm strips onto the scratched surface of the glass slides by using scotch tape (3M) as a spacer. After drying under ambient air, the films were heated to 500℃ in stages in a programmable furnace to remove the organic templates and leave a highly porous TiO_2 film. The temperature profile of the heating regime was as follows: 325℃ for 5 min, 375℃ for 5 min, 450℃ for 15 min, 500℃ for 15 min. The heating ramp rate between each stage was 10℃ min^{-1}.

Films of other shapes (2 cm * 2 cm, 2.5 cm * 2.5 cm) were also fabricated in the same way for the X-ray diffraction and diffuse reflectance characterizations. Films of 3 cm * 1 cm were prepared using the same doctor blading technique on clean FTO glass slides for Mott-Schottky analyses.

Carbon coating

N-TiO_2 films were dipped into catechol aqueous solution (5 mg·mL^{-1}) for 30 min. The films were then rinsed thoroughly with deionised water and dried under ambient air. Finally, the films were heated under N_2 on a hotplate (10 min at 200℃, 30 min at 300℃), during which time the colour of the films turns brown, indicating the thermal decomposition of the catechol-TiO_2 surface complex.

Characterization

UV/Visible diffuse reflectance of the films was measured by using a JASCO V-670 spectrophotometer with an integrating sphere attachment. X-ray powder diffraction data were acquired with a Bruker D2 phaser X ray diffractometer in reflection geometry with CuKa radiation (1.54184 Å). Data were collected over the 2θ range 5 – 60 ° for a scan time of 10 mins. SEM images were collected by using a Carl Zeiss SIGMA HD VP Field Emission SEM, operated in InLens mode with a 10kV accelerating voltage. Mott–Schottky analyses were performed using an Electrochemical Impedance Spectroscopy AUTOLAB with FRA software to control a standard three electrode setup. Ag/AgCl reference electrode and Pt wire counter electrode were used, with the film constituting the working electrode, and the electrolyte used was 0.1 M Na_2SO_4.

Photocatalytic testing

3cm * 0.9 cm TiO_2 photocatalyst films were submerged into an aqueous solution of Rhodamine B (3 mL, 1.0×10^{-5} M) in a standard UV-vis quartz cuvette. The films were stirred in the dark for 30 min to establish an adsorption equilibrium, then irradiated with a 410 nm LED (5.0 V * 0.8 A, 4 W applied power). The distance of LED and the film was fixed to 5 cm. The decolourisation of Rhodamine B was followed by measuring the absorption at 553 nm at regular time intervals using a JASCO V-670 spectrophotometer. The degradation of 4-chlorophenol was measured in the same way, using a 4-chlorophenol aqueous solution of 1.6×10^{-4} M concentration and using the absorption peak at 280 nm. Photocatalytic tests under UV were carried out in the same setting, using a 370 nm LED (5.0 V * 0.8 A, 4 W applied power). LED spectra measured by an Ocean

Optic Spectrometer can be seen in Figure S8. The system was under room temperature (24-26℃) during all the tests.

Scavenging experiment

Scavenging experiments were carried out on the same solution of Rhodamine B in regular tests, but with additional tert-butanol (TBA, 50 mM), disodium EDTA (50 mM), or bubbling N_2 as scavengers. T5NC films were used in all scavenging experiments. The decolourisation of Rhodamine B was followed by measuring the absorption at 553 nm at regular time intervals using a JASCO V-670 spectrophotometer.

Acknowledgements

The authors would like to thank Chinese Scholarship Council (Master project scholarship to Yishu Zhang) for financial support.

Keywords: titanium dioxide • photocatalysis • water purification • nitrogen doping • carbon layer

[1] The United Nations, *The United Nations World Water Development Report 2015*, **2015**.

[2] The United Nations, *The United Nations World Water Development Report 2017*, **2017**.

[3] The United Nations, *The United Nations World Water Development Report 2019*, **2019**.

[4] F. Han, V. S. R. Kambala, M. Srinivasan, D. Rajarathnam, R. Naidu, *Appl. Catal. A Gen.* **2009**, *359*, 25–40.

[5] G. Odling, N. Robertson, *ChemPhysChem* **2017**, *18*, 728–735.

[6] L. Galeano, S. Valencia, G. Restrepo, J. M. Marín, *Mater. Sci. Semicond. Process.* **2019**, *91*, 47–57.

[7] A. Alzamly, F. Hamed, T. Ramachandran, M. Bakiro, S. H. Ahmed, S. Mansour, S. Salem, K. Abdul al, N. S. Al Kaabi, M. Meetani, et al., *J. Water Reuse Desalin.* **2019**, *9*, 31–46.

[8] H. Eskandarloo, A. Badiei, M. A. Behnajady, G. Mohammadi Ziarani, *Photochem. Photobiol.* **2015**, *91*, 797–806.

[9] G. Odling, N. Robertson, *ChemPhysChem* **2016**, 2872–2880.

[10] C. Byrne, L. Moran, D. Hermosilla, N. Merayo, Á. Blanco, S. Rhatigan, S. Hinder, P. Ganguly, M. Nolan, S. C. Pillai, *Appl. Catal. B Environ.* **2019**, *246*, 266–276.

[11] M. Xu, P. Da, H. Wu, D. Zhao, G. Zheng, *Nano Lett.* **2012**, *12*, 1503–1508.

[12] M. Ben Chobba, M. Messaoud, M. L. Weththimuni, J. Bouaziz, M. Licchelli, F. De Leo, C. Urzì, *Environ. Sci. Pollut. Res.* **2019**, DOI 10.1007/s11356-019-04680-7.

[13] T. Suwannaruang, P. Kidkhunthod, N. Chanlek, S. Soontaranon, K. Wantala, *Appl. Surf. Sci.* **2019**, *478*, 1–14.

[14] D. Chen, Z. Jiang, J. Geng, Q. Wang, D. Yang, *Ind. Eng. Chem. Res.* **2007**, *46*, 2741–2746.

[15] M. Du, B. Qiu, Q. Zhu, M. Xing, J. Zhang, *Catal. Today* **2019**, *327*, 340–346.

[16] N. R. Khalid, A. Majid, M. B. Tahir, N. A. Niaz, S. Khalid, *Ceram. Int.* **2017**, *43*, 14552–14571.

[17] G. Odling, A. Ivaturi, E. Chatzisymeon, N. Robertson, *ChemCatChem* **2018**, *10*, 234–243.

[18] K. Ettrup, A. Kounina, S. F. Hansen, J. A. J. Meesters, E. B. Vea, A. Laurent, *Environ. Sci. Technol.* **2017**, *51*, 4027–4037.

[19] A. Monshi, M. R. Foroughi, M. R. Monshi, *World J. Nano Sci. Eng.* **2012**, *02*, 154–160.

[20] P. G. Smirniotis, T. Boningari, S. N. R. Inturi, *Aerosol Sci. Technol.* **2018**, *52*, 913–922.

[21] X. Cheng, X. Yu, Z. Xing, L. Yang, *Arab. J. Chem.* **2016**, *9*, S1706–S1711.

[22] G. B. Soares, B. Bravin, C. M. P. Vaz, C. Ribeiro, *Appl. Catal. B Environ.* **2011**, *106*, 287–294.

[23] L. K. Preethi, R. P. Antony, T. Mathews, S. C. J. Loo, L. H. Wong, S. Dash, A. K. Tyagi, *Int. J. Hydrogen Energy* **2016**, *41*, 5865–5877.

[24] S. S. Abdullahi, S. Güner, Y. Koseoglu, I. Murtala, B. I. Adamu, M. I. Abdulhamid, *J. Niger. Assoc. Math. Phys.* **2016**, *35*, 241–246.

[25] R. López, R. Gómez, *J. Sol-Gel Sci. Technol.* **2012**, *61*, 1–7.

[26] K. Gelderman, L. Lee, S. W. Donne, *J. Chem. Educ.* **2007**, *84*, 685–688.

[27] H. Kisch, *Angew. Chemie - Int. Ed.* **2010**, *49*, 9588–9589.

[28] H. Kisch, D. Bahnemann, *J. Phys. Chem. Lett.* **2015**, *6*, 1907–1910.

[29] H. Li, Y. Hao, H. Lu, L. Liang, Y. Wang, J. Qiu, X. Shi, Y. Wang, J. Yao, *Appl. Surf. Sci.* **2015**, *344*, 112–118.

[30] J. G. Mahy, V. Cerfontaine, D. Poelman, F. Devred, E. M. Gaigneaux, B. Heinrichs, S. D. Lambert, *Materials (Basel).* **2018**, *11*, 1–20.

[31] G. Li, B. Zou, S. Feng, H. Shi, K. Liao, Y. Wang, W. Wang, G. Zhang, *Phys. B Condens. Matter* **2020**, 412184.

Entry for the Table of Contents

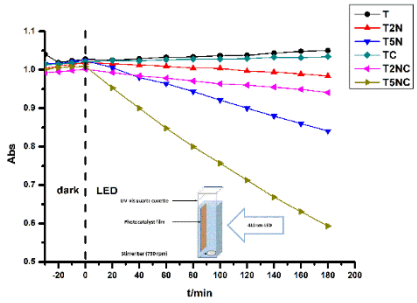

C-coated N-doped TiO_2 on glass substrates showed higher photocatalytic efficiency than TiO_2 for degrading Rhodamine B but was ineffective for degrading 4-chlorophenol. This emphasises the need for a varied scope of model pollutants in photocatalytic water treatment experiments.